Journal of Power Sources 195 (2010) 7445–7451

Contents lists available at ScienceDirect

Journal of Power Sources

journal homepage: www.elsevier.com/locate/jpowsour

Physical and electrochemical properties of $LiMnPO_4$/C composite cathode prepared with different conductive carbons

Zhumabay Bakenov, Izumi Taniguchi*

Department of Chemical Engineering, Tokyo Institute of Technology, 2-12-1 Ookayama, Meguro-ku, Tokyo 152-8552, Japan

ARTICLE INFO

Article history:
Received 8 April 2010
Received in revised form 7 May 2010
Accepted 11 May 2010
Available online 19 May 2010

Keywords:
$LiMnPO_4$/C composites
Conductive carbon
Spray pyrolysis
Wet ballmilling

ABSTRACT

The olivine structured $LiMnPO_4$/C composites were prepared by a combination of spray pyrolysis and wet ballmilling using different conductive carbons: acetylene black and two types of ketjen black. The ketjen black with a larger specific surface area and dibutyl phthalate absorption number was found to be more preferable compared with other conductive carbons studied in this work. The $LiMnPO_4$/C composite cathode with ketjen black, which has the largest specific surface area, exhibited the largest discharge capacity compared with other $LiMnPO_4$/C composites. The largest discharge capacity delivered by this composite cathode was 166 mAh g^{-1} at 0.05 C, which is about 97% of the theoretical value for $LiMnPO_4$. The performance improvement by using this conductive carbon was attributed to its extremely large specific surface area and high ability to absorb the electrolyte, which provide enhanced charge transfer and lithium ion transport in the composite cathode structure.

1. Introduction

Secondary Li-ion batteries (LIBs) are dominating the market of portable electronics and expanding its application for the electricity powered transportation [1]. Despite this, the serious barriers for its wider use in large scale devices such as car batteries and stationary energy storage systems remain the high cost and toxicity of the LIBs materials, especially, the Co-based cathode materials. The olivine $LiMPO_4$ (M = Fe, Mn) phosphates are an ideal replacement for these cathodes due to its low cost, non-toxicity, large theoretical capacity, and thermal and electrochemical stabilities [2–6]. However, intrinsic low ionic and electronic conductivities of $LiMPO_4$ restrict achieving high electrochemical activities. This disadvantage has been successfully overcome in case of $LiFePO_4$ by the preparation of nanosized powders and conductive coating of the particle surface [2,7,8], and these nanoparticles exhibit a discharge capacity close to its theoretical value. $LiMnPO_4$ is more attractive than $LiFePO_4$ due to its higher operating voltage of 4.1 V. However, $LiMnPO_4$ still remains a challenge for researchers to be developed to the level of practical cathode for LIBs. Various synthetic routes were applied to prepare high-performance $LiMnPO_4$ cathode [4,5,9,10]. Preparation of nanostructured $LiMnPO_4$/C composite particles and conductive carbon addition during its synthesis were used to compensate its low conductivity [5,9–11]. These allowed the performance improvement of $LiMnPO_4$ cathode material. Up to date the largest discharge capacity for $LiMnPO_4$ has been reported to be 149 mAh g^{-1} at 0.1 C in the galvanostatic charge–discharge [5], which is about 87% of the theoretical value of 171 mAh g^{-1}. For the trickle charge mode conditions, the initial discharge capacity was reported to be about 130 mAh g^{-1} at 0.1 C discharge rate [4,5,8,9], which is far below of the theoretical capacity of $LiMnPO_4$. Therefore, further investigations to improve the electrochemical performance of $LiMnPO_4$ cathode are crucial. From this point of view, the investigation of the effect of different conductive carbons used in the $LiMnPO_4$/C composite on its electrochemical properties is very important [12–18]. Both the abilities of the conductive carbon to conduct electrons and transport lithium ions are crucial for the electrochemical performance of the composite cathodes. Different carbon additives have different physical properties such as particle size, absorption ability and specific surface area. Each of these characteristics of the conductive carbon might have a significant effect on the overall conductivity of the electrode, the electrolyte absorption and, as a result, influence the overall electrochemical performance of the cell. Jin et al. [12] reported that acetylene black (AB) is preferable as a conductive agent for $LiCoPO_4$ cathode compared with carbon black, and the cathode with AB shows better electrochemical performance. It was suggested by Choi et al. [13] that the dibutyl phthalate (DBP) absorption number should be considered more significantly when selecting the carbon black for the cathode mixture. Kuroda et al. [14] studied the effect of different conductive carbons such as ketjen black (KB), AB, and graphite on the electrochemical performance of $LiCoO_2$ cathode. Among other conductive carbons, KB has a larger surface area and DBP

* Corresponding author. Tel.: +81 3 5734 2155; fax: +81 3 5734 2155.
E-mail addresses: taniguchi.i.aa@m.titech.ac.jp, itaniguc@chemeng.titech.ac.jp (I. Taniguchi).

0378-7753/$ – see front matter © 2010 Elsevier B.V. All rights reserved.
doi:10.1016/j.jpowsour.2010.05.023

adsorption number, and the composite electrode used this conductive carbon had an enhanced performance due to the extremely high mesopore area and electrical conductivity of KB [14]. It was shown that a large mesopore specific surface area of carbon could provide favorable and quick pathways for ions to penetrate [15], and the electrolyte adsorbed mesopore carbon provides intimate contact between lithium ions and the cathode material particles and improves the composite cathode conductivity [16]. Therefore, a high conductive carbon with larger specific surface area and mesopore structure could be preferable choice when selecting a better conductive agent to formulate a composite cathode for the LIBs application.

In our previous works [2,3,5,11,17], we have successfully prepared the $LiMPO_4$/C (M = Fe, Mn) composites by a combination of spray pyrolysis (SP) and ballmilling (BM) with AB as a conductive carbon. It was shown that a combination of SP and BM is a versatile method to obtain a high performance olivine structured cathodes for LIBs. In the present work, we report on the preparation of $LiMnPO_4$/C composites by a combination of SP and wet ballmilling (WBM) with different conductive carbons and study its physical and electrochemical properties.

2. Experimental

Schematic diagrams of the SP facility and powder preparation have been described elsewhere [18,19]. A stoichiometric ratio of $LiNO_3$ (98%), $Mn(NO_3)_2{\cdot}6H_2O$ (98%) and H_3PO_4 (85% solution, all from Wako Pure Chemical Industries) were dissolved in distilled water with a total concentration of 0.6 mol L^{-1} and used as a precursor solution for SP in a tubular furnace at 400 °C in a $N_2 + 3\%H_2$ atmosphere. The as-prepared powder was milled with ethanol and 20 wt.% of conductive carbon: AB (DENKA BLACK, Denki Kagaku Kogyo Kabushiki Kaisha, Japan) and two types of KB (EC300J and EC600JD, both from Ketjen Black International Company, Japan), denoted further as KB1 and KB2, at 800 rpm for 6 h in a zirconia vessel using zirconia balls. The WBM samples were thereafter heat-treated in a tubular furnace at 500 °C for 4 h in a $N_2 + 3\%H_2$ gas. Physical properties of the final samples ($LiMnPO_4$/C, C = AB, KB1, KB2) were examined by X-ray diffraction analysis (XRD; Rigaku, Ultima IV with D/teX Ultra) using CuKα radiation with a scan speed of 5° min^{-1} ranging from 10° to 70°, field-emission scanning electron microscopy (FE-SEM, Hitachi, S-800) operated at 8 kV, and transmission electronic microscopy (TEM, JEM-200CX, JEOL, Ltd.). The geometric mean diameter, $d_{g,p}$, and geometric standard deviation, σ_g, were determined by randomly sampling around 500 particles from the SEM pictures from the equations:

$$\ln d_{g,p} = \frac{\sum_{i=1}^{N} \ln d_i}{N} \quad (1)$$

$$\ln \sigma_g = \left[\frac{\sum_{i=1}^{N} \left(\ln d_i - \ln d_{g,p} \right)^2}{N-1} \right]^{1/2} \quad (2)$$

respectively, in which N is the total sample number. The specific surface area was determined by the Brunauer–Emmett–Teller (BET) method (Shimadzu, Flow Sorb II 2300). The lattice parameters of the materials were refined by Rietveld analysis using an integrated X-ray Powder Diffraction Software Package PDXL (Rigaku, Version 1.3.0.0). The carbon content was analyzed by CHN Corder (MT-6, YANACO). The cathode was prepared by coating of a slurry of $LiMnPO_4$, polyvinylidene fluoride and conductive carbon in a total weight ratio of 70:10:20 onto an aluminum foil, which thereafter was dried at 110 °C in a vacuum oven for 6 h, cut into circles and assembled in the lithium coin-cell (CR2032). It should be noted that the composite electrodes with different conductive carbons were prepared to make their weight and thickness the same by precise weighing and roll pressing, and the active surface area of all electrodes was equal to 1 cm^2. The thickness of electrode was approximately 20 μm and the mass of active material in the composite electrode was approximately 1 mg. These measures were supposed to reduce the errors of the comparison of the cyclic voltammetry (CV) and ac impedance data for different electrodes [20,21]. A 1 M $LiPF_6$ solution in ethylene carbonate–diethyl carbonate (EC:DEC = 1:1, Tomiyama Pure Chemical) was used as the electrolyte. The cells were assembled in the high purity argon filled dry box, and cycled at various C rates (1 C = 171 mAh g^{-1}) galvanostatically and under the trickle charge mode in the cutoff ranges 2.5–4.4 and 2.5–4.9 V *vs* Li^+/Li at room temperature. CV was measured between 2.5 and 4.4 V using the Solartron SI 1287 electrochemical interface with a scan rate of 0.1 mV s^{-1}. The same facility was used for the ac impedance spectroscopy (AIS) measurements by applying an ac voltage of 10 mV over the frequency range from 0.1 Hz to 1 MHz. The AIS data fitting was performed using the ZPlot software (Scribner Associates, Inc.). All the electrochemical measurements were carried out in three parallel cells to ensure data reproducibility.

Table 2
Refined lattice parameters of $LiMnPO_4$/C (C = AB, KB1 and KB2) composites materials prepared by a combination of SP and WBM.

Carbon composite	a (Å)	b (Å)	c (Å)	Volume (Å^3)	χ^2
$LiMnPO_4$/AB	6.1011(3)	10.4490(2)	4.7441(7)	302.444	1.6
$LiMnPO_4$/KB1	6.1016(4)	10.4493(2)	4.7442(6)	302.509	1.5
$LiMnPO_4$/KB2	6.1026(4)	10.4487(7)	4.7447(3)	302.524	1.3

3. Results and discussion

3.1. Materials characterization

Table 1 presents the physical properties of the conductive carbon powders used in this work to prepare the $LiMnPO_4$/C composites. While the average particle size decreases in the series AB–KB1–KB2, the specific surface area and DBP absorption number drastically increase, and for KB2 these characteristics are about 21 and 3 times larger, respectively, than that of AB.

The XRD data (Fig. 1) has confirmed the single phase orthorhombic structure with a *Pnmb* space group of the $LiMnPO_4$/C composites (C = AB, KB1 and KB2) prepared in this work, and all the XRD peaks could be indexed respectively. The refined lattice parameters (ICDD 33-0804) of these composite materials are presented in Table 2 along with the goodness of fit χ^2, which is the square of the stan-

Table 1
Physical properties of conductive carbon powders used to prepare the $LiMnPO_4$/C composites.

Conductive carbon	Average primary particle size (nm)	BET surface area (m^2 g^{-1})	DBP adsorption number (cm^3 100 g^{-1})
AB	35	68	175
KB-1 (EC300J)	40	800	365
KB-2 (EC600JD)	34	1400	495

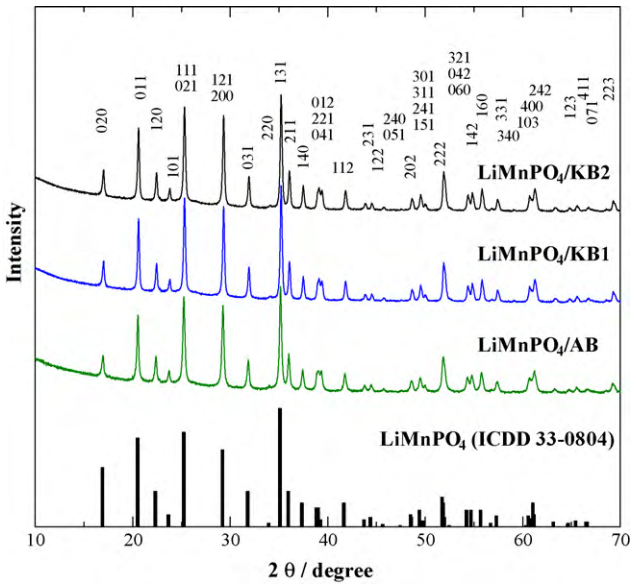

Fig. 1. XRD spectra of $LiMnPO_4$/C (C = AB, KB1 and KB2) composite materials.

dard deviation between the experimental data and the calculated parameters:

$$\chi^2 = \left(\frac{R_{wp}}{R_{\exp}}\right)^2 \quad (3)$$

The lattice parameters agree well with the literature data [9,10,22].

Fig. 2 presents the FE-SEM images of the as-prepared $LiMnPO_4$ and the $LiMnPO_4$/C composites prepared by a combination of SP and WBM. It can be seen that the as-prepared $LiMnPO_4$ consists of spherical particles. After WBM with different conductive carbon additives, the nanosized powders of the $LiMnPO_4$/C composites were formed. The particle size distribution of the as-prepared $LiMnPO_4$ and $LiMnPO_4$/C composites is shown in Fig. 3. The powders have a narrow particle size distribution. The geometric mean diameter of the as-prepared $LiMnPO_4$ is about 1 μm (Fig. 3a) while for the carbon composites this value is about 100 nm. The geometric mean diameter of the as-prepared $LiMnPO_4$ has become about one-tenth in the WBM process (Fig. 3b–d). The TEM observation data of $LiMnPO_4$/C (C = KB2) are presented in Fig. 4. From the TEM images, one can confirm that the $LiMnPO_4$/C composite can be successfully prepared by the present method. The average particle size of the composites is about 100 nm. The carbon content was about 20 wt.% in all the $LiMnPO_4$/C (C = AB, KB1, KB2) composites.

The BET specific surface area of the as-prepared $LiMnPO_4$ was about 4 $m^2\,g^{-1}$. For the $LiMnPO_4$/C (C = AB, KB1, KB2) composites, the specific surface area was 69, 73, and 87 $m^2\,g^{-1}$ for AB, KB1, and KB2, respectively. The change in the specific surface area of the $LiMnPO_4$/C (C = AB, KB1, KB2) composites follows the change in the specific surface area of the conductive carbons (Table 1). As expected, the largest specific surface area was shown by the KB2 added composite material, because of the largest specific surface area of KB2 itself compared with other conductive carbons used in this work.

3.2. Electrochemical properties of the $LiMnPO_4$/C composite cathode

Fig. 5 shows the initial discharge profiles of the $LiMnPO_4$/C (C = AB, KB1, KB2) composites prepared by a combination of SP

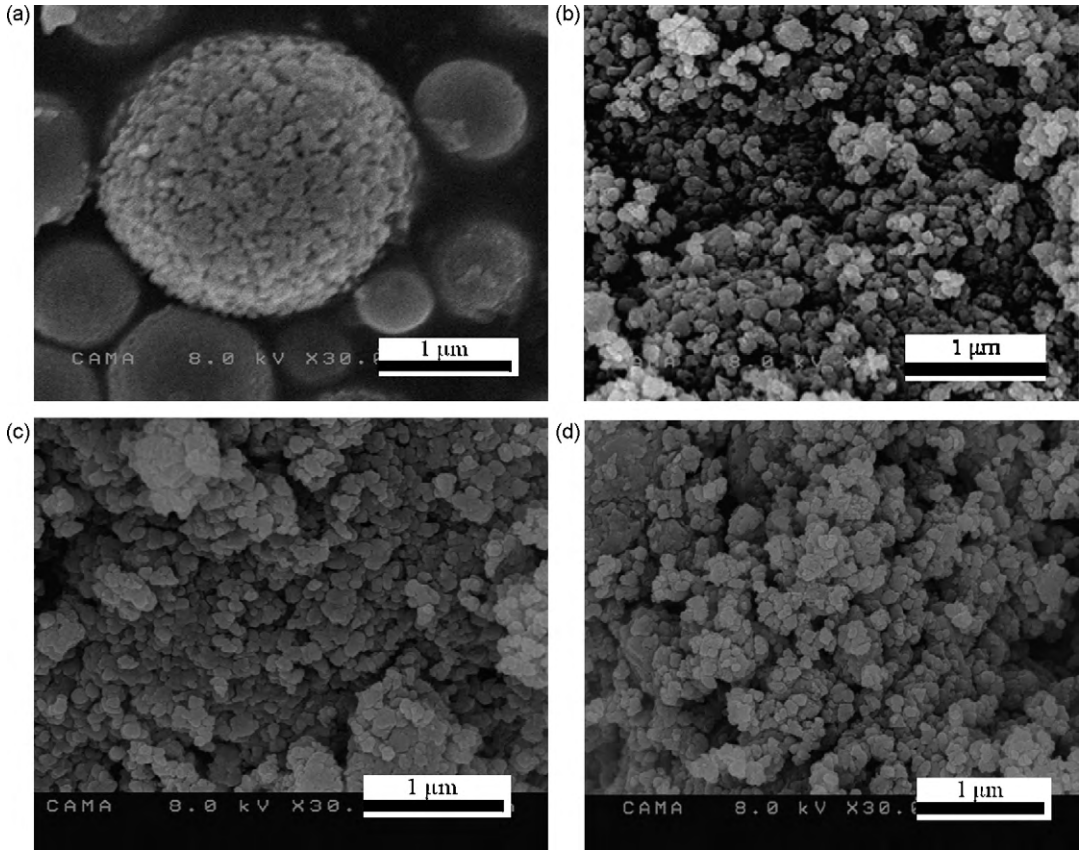

Fig. 2. FE-SEM images of (a) as-prepared $LiMnPO_4$, (b) $LiMnPO_4$/AB, (c) $LiMnPO_4$/KB1 and (d) $LiMnPO_4$/KB2 composite materials.

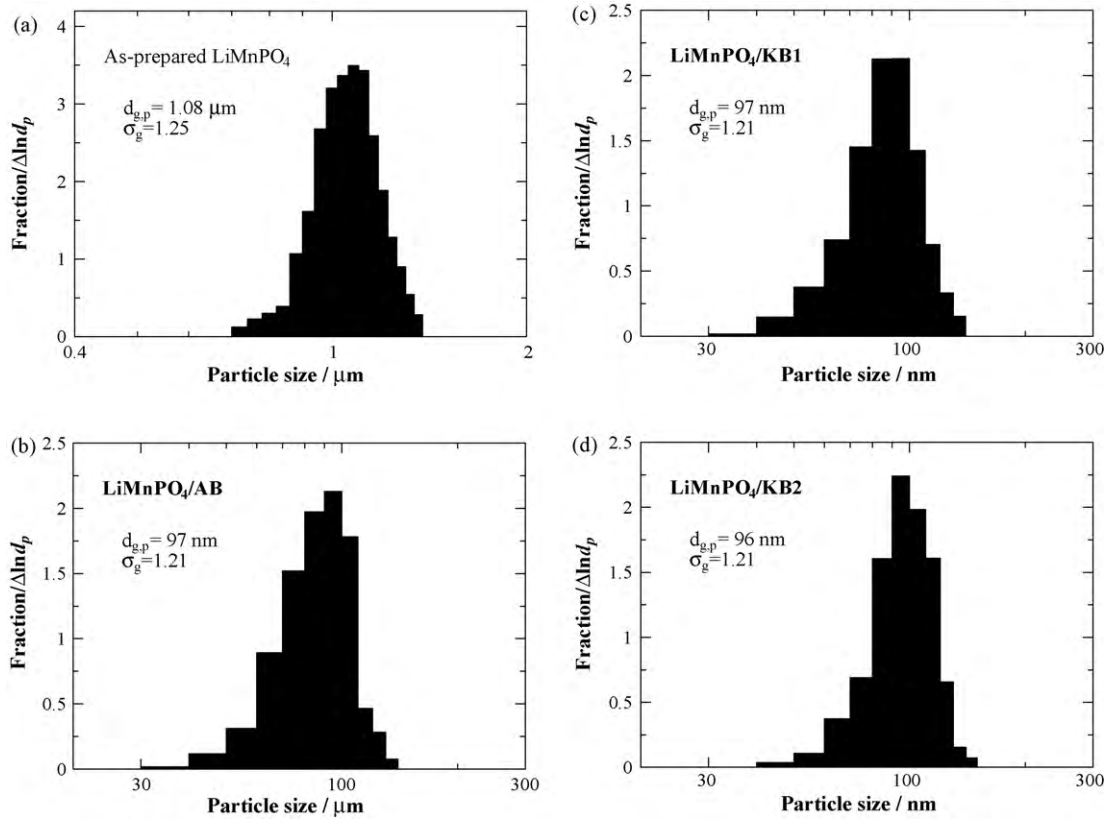

Fig. 3. Particle size distribution of (a) as-prepared $LiMnPO_4$, and (b) $LiMnPO_4$/AB, (c) $LiMnPO_4$/KB1, and (d) $LiMnPO_4$/KB2 composite materials.

and WBM at a galvanostatic charge–discharge 0.05 C rate. The initial discharge capacity of the composite cathode changes in the same manner as the specific surface area and/or DBP absorption numbers of the conductive carbon, and the composite cathode with KB2 showed the largest discharge capacity of 111 mAh g^{-1}. In order to clarify the difference in the electrochemical response of the electrode materials, the CV examination of the $LiMnPO_4$/C composites with different conductive carbons was carried out. Electrochemical responses of the $LiMnPO_4$/C cells during the CV measurements are presented in Fig. 6a. It shows the electrochemical processes in the Mn^{3+}/Mn^{2+} region at approximately 4.1 V and corresponds to the data shown in Fig. 5. The peak intensities increase in the AB–KB1–KB2 series, which could indicate the kinetic improvements [12,23] and agree well with the electrochemical performance improvement in this series. Fig. 6b presents the ac impedance spectra for the studied composite cathodes in the fresh lithium cell with an open circuit voltage of approximately 3.1 V. The AIS spectra are represented by a compressed semicircle in high-to-medium frequency range, and a declined line of the Warburg impedance in low frequency region. The studied $LiMnPO_4$/C composites consist of multiple interfaces and phase boundaries, and the complex impedance analysis is complicated. However, some simple suggestions can be made on the basis of approaches developed in our previous work [17] and reported for the similar systems in the literature [4]. The equivalent circuit fitting was applied to the AIS data. Fig. 6c represents the best fitting equivalent circuit, which could be represented as follows:

$$R_s(R_1\mathrm{CPE}_1)(R_2\mathrm{CPE}_2)W_o \quad (4)$$

where R_s is a resistance associated with the impedance of the electrolyte and consistent with the high frequency intercept in the ac impedance spectra; $(R_1\mathrm{CPE}_1)(R_2\mathrm{CPE}_2)$ is a component of the ac impedance semicircle in high-to-medium frequency range consisting of charge transfer resistances R_i and constant phase elements CPE_i; and W_o is a Warburg element corresponded to the Li-ion diffusion in the bulk of the electrode.

For the composite electrodes containing highly conductive carbon coated $LiMnPO_4$ nanoparticles, the semicircle in the high-to-medium frequency range could be attributed to the complex impedance of charge transfer from electrolyte to electrode active mass [4,17] through the solid electrolyte interface (SEI) formed on the electrodes surface, the $LiMnPO_4$ particle-to-particle resistance and the capacitances related to these processes [4,18]. The inclined line in the lower frequency range is attributed to the Warburg impedance and could be responsible for the lithium ion diffusion in the $LiMnPO_4$ particles. The diameter of the semicircle in high-to-medium frequency range is the smallest for the composite cathode with KB2, and the Warburg component of the spectra of this system has a bigger slop compared with that of the composites with KB1 and AB. These could indicate the enhanced charge transfer and lithium ion conduction in $LiMnPO_4$/KB2 composite cathode, which agrees with the charge–discharge (Fig. 5) and CV (Fig. 6a) data, and could be one of the main reasons of the improved discharge capacity of the composite cathode with KB2 compared with the cathodes containing AB and KB1 as a conductive carbon. Upon cycling, the impedance semicircle diameter increases for all the composite cathodes (not shown), which is typical for many insertion composite electrodes and could be attributed to the surface film growth upon cycling. The calculated impedance profiles are plotted in Fig. 6b and fit with the experimental data. The impedance measurements were carried out for the fresh cells, which were fully charged up to 4.4 V and fully discharged down to 2.5 V, and in each charged and discharged states, respectively. It was found that the changes in the impedance response have the same trends when measured in both the charged and discharged states. The R_s, R_i and CPE values derived from the equivalent circuit fitting are

Table 3
Impedance parameters derived from equivalent circuit for $LiMnPO_4$/C (C = AB, KB1, KB2) composites in fresh cell and discharged cell after three charge–discharge cycles.

Conductive carbon	R_s (Ω)	R_1 (Ω)	CPE_1-T ($\times 10^{-6}$) (F)	R_2 (Ω)	CPE_2-T ($\times 10^{-5}$) (F)
AB					
Fresh cell	3.391	2.975	1.184	212.2	3.774
Cell after three cycles	3.359	4.266	1.505	667.3	1.586
KB1					
Fresh cell	3.359	4.154	1.467	163.3	5.224
Cell after three cycles	3.363	3.969	3.779	294.4	4.748
KB2					
Fresh cell	3.278	3.968	3.275	154.6	4.018
Cell after three cycles	3.356	3.692	6.583	259.3	2.867

presented in Table 3 for a fresh and cell after three cycles with $LiMnPO_4$/C (C = AB, KB1, KB2) composite cathodes in the discharged state (2.5 V). The constant phase element consists of two parameters, CPE_i-T and CPE_i-P. The CPE_i-P parameter for both CPE_1 and CPE_2 for all samples varies from 0.6 to 0.9 F and does not remarkable change upon the cell operation. Therefore, only its CPE_i-T parameter of CPE is presented in Table 3. The R_s values for all composite cathodes are close to each other and do not remarkably change upon cycling. One can see that the R_2 is much larger than R_1 for all composite cathodes; therefore, only R_2 value could be used in the charge transfer impedance evaluation. Furthermore, R_2 is the most drastically changing impedance parameter upon cycling, especially for the $LiMnPO_4$/AB composite cathode. The increase of charge transfer resistance with cycle number may be due to the formation of passive films upon the cell operation and could be responsible for the cell electrochemical performance change during cycling.

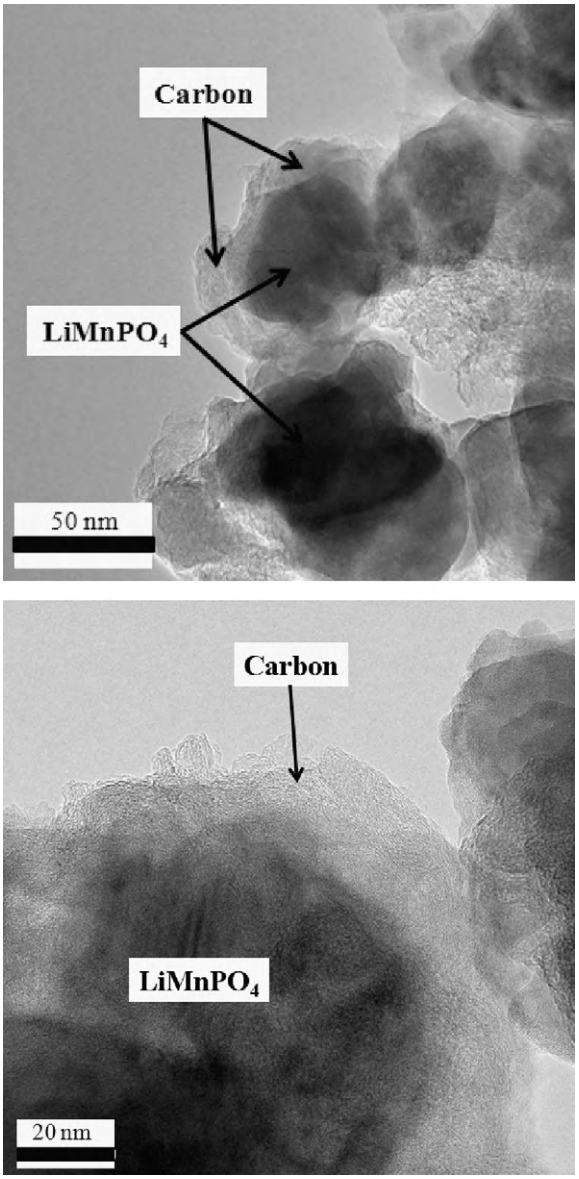

Fig. 4. TEM images of $LiMnPO_4$/KB2 composite materials.

The electrochemical performance for the composite cathodes with different conductive carbons could be affected by the difference in both the specific surface area of the composite cathodes and the DBP absorption number of the conductive carbons used to prepare the composites. Both of these characteristics might favor the improvement of the electrochemical performance of the cell by increasing the electronic and ionic conductivity of the cathode. KB1 and KB2 have a large mesopore surface area and a higher DBP absorption number compared with AB. Therefore, the $LiMnPO_4$/C composite cathodes with these conductive carbons have a high ability to absorb the electrolyte and provide easy penetration and quick Li-ion transport into the electrode structure [13–16]. As it was mentioned above, KB2 has 21 and 3 times larger specific surface area and DBP absorption number, respectively, than AB, and remarkably larger than that of KB1. Our studies on the electrochemical performance have shown that KB2 is more preferable as a conductive additive to prepare $LiMnPO_4$/C composite cathode than AB and KB1.

In our previous work [5,17], we reported that the $LiMnPO_4$/C composite cathodes prepared by a combination of SP and WBM exhibited enhanced electrochemical performance when charged to a higher cutoff voltage of 4.9 V. The composite cathode with KB2

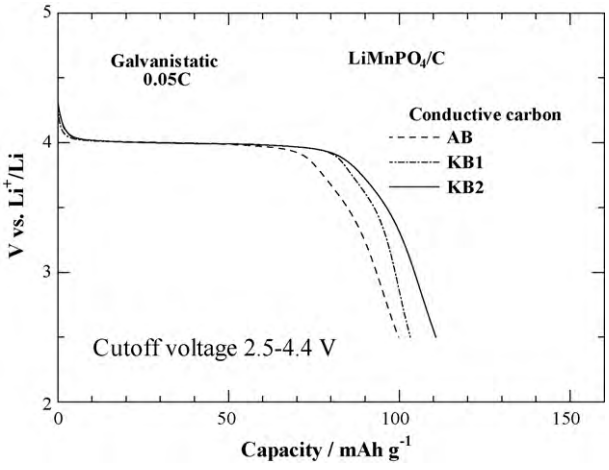

Fig. 5. Initial discharge profiles of $LiMnPO_4$/C (C = AB, KB1, KB2) composites cathodes. Galvanostatic charge–discharge at 0.05 C. Cutoff voltage 2.5–4.4 V.

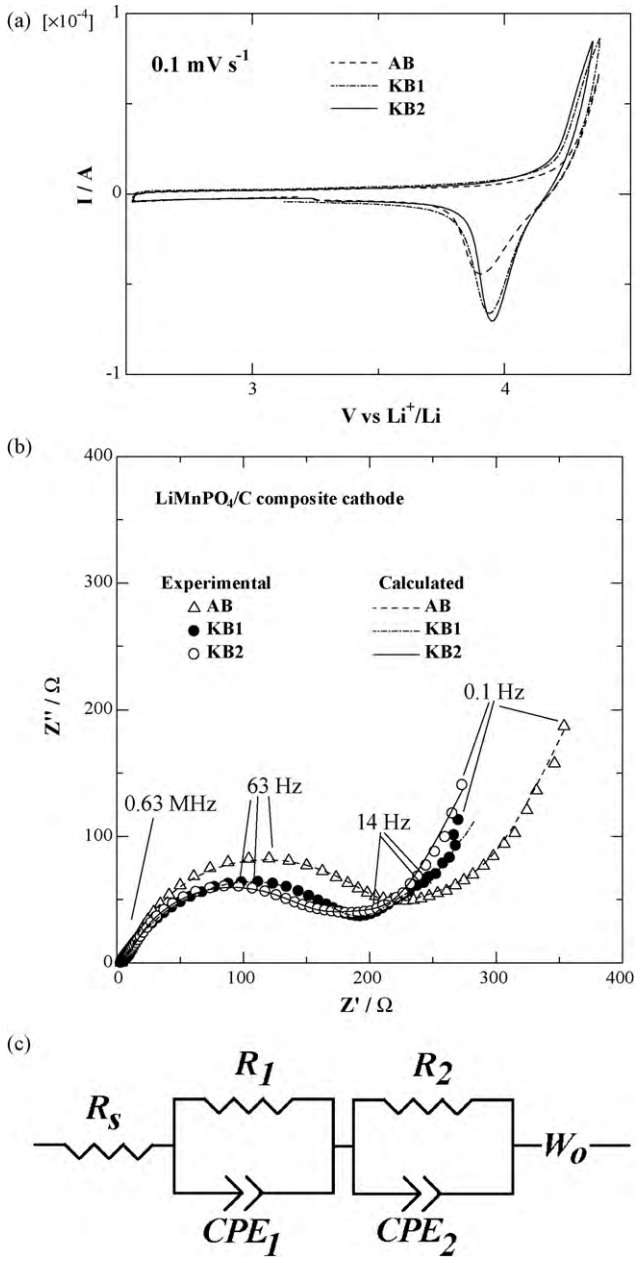

Fig. 6. (a) Cyclic voltammogram, scan rate: 0.1 mV s^{-1}, (b) AIS spectra of $LiMnPO_4$/C (C = AB, KB1 and KB2) composite cathodes prepared with different conductive carbon additives in fresh lithium cell, and (c) equivalent circuit model of the studied systems.

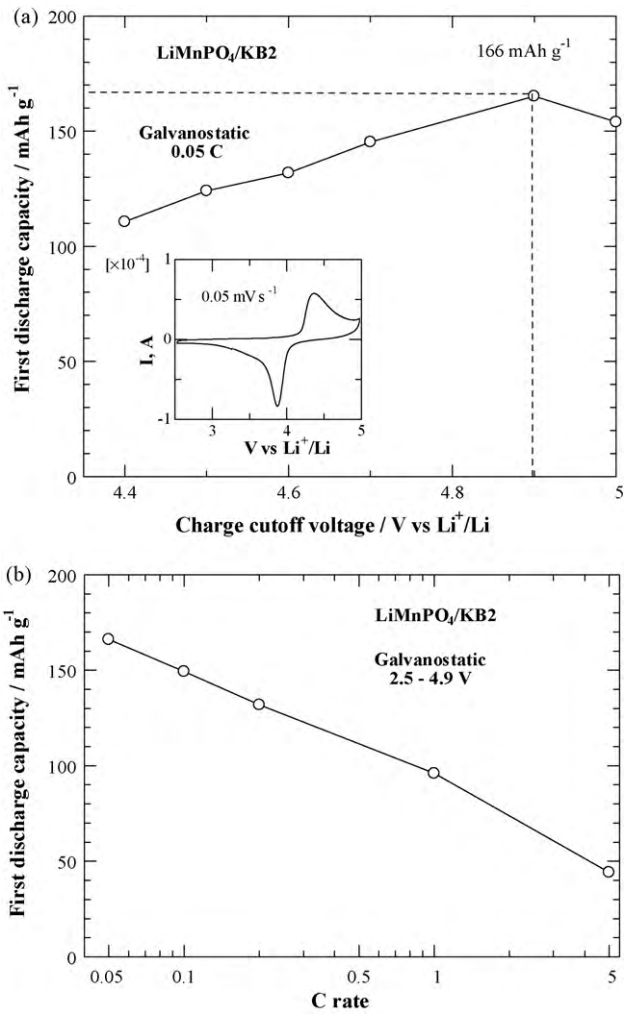

Fig. 7. (a) Effect of charge cutoff voltage on the initial discharge capacity of $LiMnPO_4$/KB2 composite cathode at galvanostatic charge–discharge, 0.05 C; inset: initial CV curve of $LiMnPO_4$/KB2, scan rate 0.05 mV s^{-1}. (b) Rate capability of $LiMnPO_4$/KB2 composite cathode at cutoff voltage 2.5–4.9 V.

was examined in these conditions. Fig. 7a exhibits the effect of the higher cutoff voltage on the initial discharge capacity of the composite cathode. The discharge capacity of $LiMnPO_4$/KB2 was remarkably increased by increasing the charge cutoff voltage, and the largest discharge capacity of 166 mAh g^{-1} was achieved when the cell was charged to 4.9 V. This is about 97% of the theoretical discharge capacity of $LiMnPO_4$ and the largest value reported to date in the literature for this material. Further increase of the cutoff voltage up to 5 V led to the discharge capacity decrease. This phenomenon might be attributed to the electrolyte decomposition at the potentials close to 5 V [17], although the corresponding processes were not observed in the CV measurements from 2.5 to 5 V presented in the inset of Fig. 7a. Fig. 7b presents the rate capability data for the $LiMnPO_4$/KB2 composite cathode at 2.5–4.9 V cutoff voltages. Fig. 8 shows the cell cyclability at 0.2 C of galvanostatic charge-discharge to 4.9 V. It can be seen that the $LiMnPO_4$/KB2 composite cathode has good cyclability and rate capability.

The electrochemical properties of $LiMnPO_4$/KB2 composite cathode were also examined in the trickle charge mode conditions.

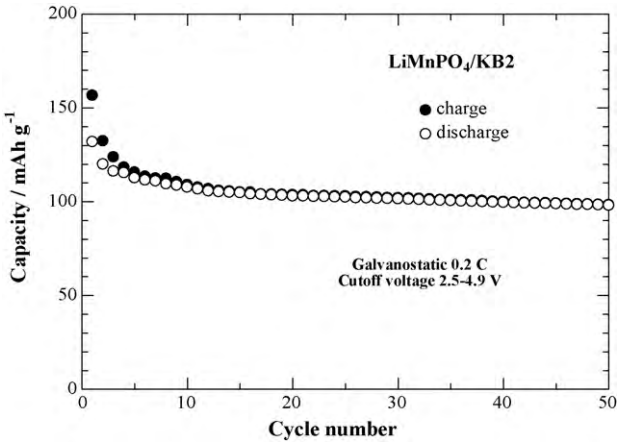

Fig. 8. Cycling performance of $LiMnPO_4$/KB2 composite cathode at galvanostatic charge–discharge, 0.2 C. Cutoff voltage 4.9 V.

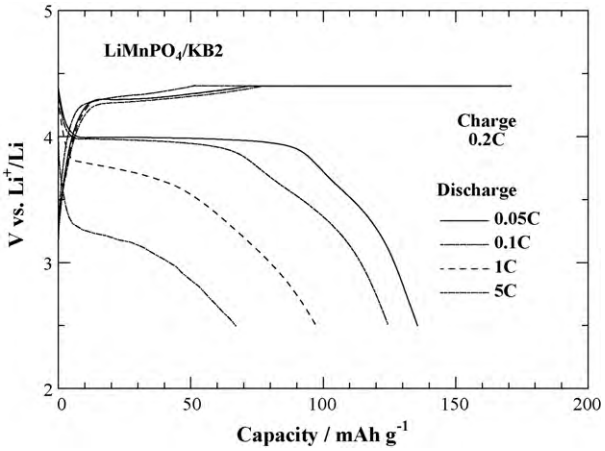

Fig. 9. Electrochemical performance of the $LiMnPO_4$/KB2 composite cathode under trickle charge mode conditions. Charge at 0.2 C to 4.4 V until 171 mAh g^{-1}, discharge at 0.05, 0.1, 1 and 5 C.

The cell was galvanostatically charged at 0.2 C to 4.4 V, and kept at 4.4 V until 1 C (171 mAh g^{-1}), and then galvanostatically discharged at various C rates. Fig. 9 shows the initial charge–discharge profiles of the $LiMnPO_4$/KB2 composite cathode at 0.05, 0.1, 1, and 5 C discharge rates. The composite electrode delivers a large discharge capacity along with a good rate capability.

4. Conclusions

The olivine structured $LiMnPO_4$/C composites were prepared by a combination of SP and WBM using three types of conductive carbon: AB, KB1 and KB2. The $LiMnPO_4$ nanoparticles with a narrow particle size distribution were obtained.

The use of the conductive carbon, KB2, with a larger specific surface area and DBP absorption number resulted in a larger specific surface area of the $LiMnPO_4$/KB2 composite cathode. The composite cathode with KB2 exhibited the largest discharge capacity compared with the composite cathodes with AB and KB1. The $LiMnPO_4$/KB2 composite cathode delivered the discharge capacity of 166 mAh g^{-1} at 0.05 C in the galvanostatic charge–discharge, which is about 97% of the theoretical value for $LiMnPO_4$. It also exhibited a good rate capability and cyclability. The performance improvement by using KB2 was attributed to its extremely large specific surface area and high DBP absorption number, which provides conditions for enhanced charge transfer and Li-ion diffusion. This suggestion was supported by the CV and AIS data.

Acknowledgments

This research was supported by the Development of an Electric Energy Storage System for Grid Connection with New Energy Resources under the New Energy and Industrial Technology Development Organization. The authors are grateful to the staff members of the Center for Advanced Materials Analysis (Tokyo Institute of Technology, Japan) Mr. J. Koki and Mr. K. Hori for help in the electronic microscopy observation of prepared powders.

References

[1] A.S. Aricò, P. Bruce, B. Scrosati, J.M. Tarascon, W. van Schalkwijk, Nat. Mater. (2005) 366.
[2] M. Konarova, I. Taniguchi, J. Power Sources 195 (2010) 3661.
[3] M. Konarova, I. Taniguchi, J. Power Sources 194 (2009) 1029.
[4] S.K. Martha, B. Markovsky, J. Grinblat, Y. Gofer, O. Haik, E. Zinigrad, D. Aurbach, T. Drezen, D. Wang, G. Deghenghi, J. Exnar, J. Electrochem. Soc. 156 (2009) A541.
[5] Z. Bakenov, I. Taniguchi, Electrochem. Commun. 12 (2010) 75.
[6] P.S. Herle, B. Ellis, N. Coombs, L.F. Nazar, Nat. Mater. 3 (2004) 147.
[7] B. Kang, G. Ceder, Nature 458 (2009) 190.
[8] G. Wang, Y. Cheng, M. Yan, Z. Jiang, J. Solid State Electrochem. 11 (2007) 457.
[9] T. Shiratsuchi, S. Okada, T. Doi, J. Yamaki, Electrochim. Acta 54 (2009) 3145.
[10] G. Chen, J.D. Wilcox, T.J. Richardson, Electrochem. Solid-State Lett. 11 (2008) A190.
[11] T.N.L. Doan, Z. Bakenov, I. Taniguchi, Adv. Powder Technol. 21 (2010) 187.
[12] B. Jin, H.B. Gu, K.W. Kim, J. Solid State Electrochem. 12 (2008) 105.
[13] Y.S. Choi, S. Kim, S.S. Choi, J.S. Han, J.D. Kim, S.E. Jeon, B.H. Jung, Electrochim. Acta 50 (2004) 833.
[14] S. Kuroda, N. Tobori, M. Sakuraba, Y. Sato, J. Power Sources 119–121 (2003) 924.
[15] W. Xing, S.Z. Qiao, R.G. Ding, F. Li, G.Q. Lu, Z.F. Yan, H.M. Cheng, Carbon 44 (2006) 216.
[16] Q. Zhang, G. Peng, G. Wang, M. Qu, Z.L. Yu, Solid State Ionics 180 (2009) 698.
[17] Z. Bakenov, I. Taniguchi, J. Electrochem. Soc. 157 (2010) A430.
[18] Z. Bakenov, I. Taniguchi, Solid State Ionics 176 (2005) 1027.
[19] I. Taniguchi, Mater. Chem. Phys. 92 (2005) 172.
[20] M.D. Levi, D. Aurbach, J. Phys. Chem. B 101 (1997) 4630.
[21] M.D. Levi, D. Aurbach, J. Phys. Chem. B 108 (2004) 11693.
[22] S. Geller, J.L. Durand, Acta Crystallogr. 13 (1960) 325.
[23] J.F. Ni, H.H. Zhou, J.T. Chen, X.X. Zhang, Mater. Lett. 59 (2005) 2361.